Nonlinear identification of a minimal NeuroMuscular Blockade model in anaesthesia

Margarida Martins da Silva, Torbjörn Wigren, *Senior Member, IEEE,* and Teresa Mendonça, *Member, IEEE*

Abstract

The paper presents new modeling and identification strategies to address the many difficulties in the identification of anaesthesia dynamics. During general anaesthesia procedures muscle relaxants are drugs frequently administered. The most commonly used models for the effect of such drugs, called NeuroMuscular Blockade (NMB), comprise a high number (greater than eight) of pharmacokinetic and pharmacodynamic (PK/PD) parameters. The main issue concerning the NMB system identification is that, in the clinical practice, the user cannot freely choose the system input signals (drug dose profiles to be administered to the patients) to enable the identification of such a high number of parameters. The limited amount of measurement data also indicates a need for new identification strategies. A new SISO Wiener model with two parameters is hence proposed to model the effect of the muscle relaxant *atracurium*. A batch Prediction Error Method (PEM) was first developed to optimize the model structure. Secondly, an Extended Kalman Filter (EKF) approach was used to perform the online identification of the system parameters. Both approaches outperform conventional identification strategies, showing good results regarding parameter identification and measured signal tracking, when evaluated on a large patient database. The new methods proved to be adequate for the description of the system, even with the poor input signal excitation and the few measured data samples present in this application. It turns out that the methods are of general validity for the identification of drug dynamics in the human body.

M. M. Silva is with the Faculdade de Ciências da Universidade do Porto, Rua do Campo Alegre, Porto, Portugal (e-mail: margarida.silva@fc.up.pt)

T. Wigren is with the Division of Systems and Control, Department of Information Technology, Uppsala University, Box 337, SE-751 05 Uppsala, Sweden (e-mail: torbjorn.wigren@it.uu.se)

T. Mendonça is with the Faculdade de Ciências da Universidade do Porto, Rua do Campo Alegre, Porto, Portugal (e-mail: tmendo@fc.up.pt)

Index Terms

Nonlinear system identification, Minimally parameterized models, Prediction Error Method, Extended Kalman Filter, Anaesthesia, NeuroMuscular Blockade

I. INTRODUCTION

The present paper considers nonlinear identification of the dynamics of drug effect in the human body. For this purpose, new minimally parameterized models are proposed, overcoming the poor excitation of such problems. Data collected in the surgery room from NeuroMuscular Blockade (NMB) control cases during general anaesthesia is used to exemplify the ideas.

In the clinical practice, the term anaesthesia refers to a drug-induced reversible pharmacological state where three main variables must be kept in equilibrium: *hypnosis*, *analgesia* and *areflexia*. *Hypnosis* is defined as the level of unconciousness associated with the absence of recall after surgery regarding intraoperative events. Several univariate parameters computed using the raw data from the electroencephalogram (EEG) have been used to monitor the level of hypnosis in patients, namely the spectral edge frequency [1], the auditory evoked potentials [2] and the approximate entropy [3]. More recently the Bispectral Index Scale (BIS) [4] has taken the lead, being the index most widely used by anesthetists and researchers in the field to infer the Depth of Anaesthesia (DoA). *Analgesia* is defined as the absence of pain. However, quantitative and a reliable index for the measurement of pain in patients has not yet been widely accepted and validated. Clinicians use signs as tearing, changes in the heart rate and changes in the blood pressure together to infer the analgesia condition of the patients. *Areflexia* is defined as the lack of movement. It is induced and maintained by the use of muscle relaxants and it aims to achieve an adequate level of paralysis to perform surgical procedures. The NMB level can be clinically quantified by electrical stimulation of the *adductor policies* muscle in the patient's hand. The blockade level corresponds to the first single response calibrated by a reference twitch.

In order to address the balance of these three components, the anesthetists adjust the dose of the corresponding drugs by integrating the NMB and DoA indices with all the other monitored physiological variables. When comparing with manual drug administration, automated technologies

may carry considerable advantages [5]. If reliable models of the patients' pharmacokinetics (PK) and pharmacodynamics (PD) are available, under or overdosing can be avoided by programming the syringe pumps to target specific values of the drug effects. The need to have reliable models for the patients' PK/PD benefits from the automatic identification of the patient's variability in order to overcome the drawback of using standardized procedures in drug administration based on population studies.

The application of system identification methodologies to identify the patient variability in anaesthesia environments is not understood well enough. The main problem of DoA and NMB control is the poor excitation *i.e.* the input signals (administered drug doses) are not rich enough in frequency and amplitude to be able to excite all modes of the system [6], [7]. Unfortunately, the excitatory pattern of the input cannot be chosen by the user to achieve a better performance of the identification methodologies. In general anaesthesia procedures, the induction phase usually comprises the administration of *bolus* of drugs (considered as one finite impulse) and afterwards the measured variables are kept at the desired target values by a low variance drug dose profile. Moreover, the available data is limited by the sampling rates accepted by the clinical devices.

The PK/PD of the effect of drugs in anaesthesia can be modeled as a Wiener model: a linear block in series with a nonlinear static block [8]. The linear parts describe the way the drug is diffused, accumulated and excreted by the human body. The nonlinear part models the drug effect in the patient. Due to this structure, the use of linear models to predict human response to anaesthesia is not completely adequate [9]. In [6] a first approach for reducing the number of model parameters was proposed but a linear model was used to describe the PD nonlinearity. Alternatives to the identification of linear models can be found in other publications. For example, in [10] a hybrid method based on parameter estimation and an artificial neural network coupled with a curve fitting algorithm was proposed. Good results were obtained but the parameter redundancy is still present in the calculation of the steady-state drug dose prediction. The algorithm proposed in [11] was also previously tested for the anaesthesia identification case study. The black box model approach was modified to take into account the NMB Wiener system specifications but it still failed in identifying the eight parameters present in the *atracurium* effect

model. More work in this direction is hence needed.

From the reasons stated above it is reasonable to assume that, by reducing the number of parameters to describe the system, improved results may be achieved when new system identification algorithms are designed. One strong reason for this modeling is that the input pattern present in the real collected cases will no more be insufficiently persistently exciting, making the identification possible to be carried out. The choice of the appropriate number of parameters should match the parsimony principle [12], that states that the chosen model should contain the smallest number of free parameters required to represent the true system adequately.

The main contribution of this paper is hence the use of a minimal number of parameters to model the NMB input-output relation, consistent with the poor excitation present in the available data from real cases. A nonlinear Wiener model using only two free parameters is proposed for this purpose. From this model a new batch algorithm for parameter identification is derived, providing a second contribution. The good results obtained with this first strategy act as a motivation for the development of an online adaptive algorithm by the use of the Extended Kalman Filter (EKF). This is the third contribution of the paper. Experimental evaluation of the new algorithms in a previouly collected database of sixty patients undergoing general surgery proves the feasibility of the model and the algorithms. Due to parameter adaptation, the signals achieve very good reference signal tracking in test cases, using the aforementioned database.

This paper is organized as follows. Section II describes the principles concerning the control of anaesthesia. Section III presents the definition of both the linear and the non linear parts of the new minimally parameterized model. In Section IV the batch identification algorithm using the Prediction Error Method is presented, followed by the derivation of the EKF in Section V. Sections VI and VII present optimization and simulation results, whereas Section VIII gives the conclusions.

II. Control strategies

A. Control algorithms

The first successful attempt to commercialize a device designed to control drug dose administration to patients in a personalized way was 'Diprifusor' [13]. The algorithm used by this Target-Controlled Infusion (TCI) platform receives information about the patient and then ajusts the drug dose profile in such a way as to achieve a specific predicted target effect concentration. The set of PK/PD parameters that are used to compute the drug doses were selected based on population models. Even with information regarding age, weight and height of the patient, a certain inaccuracy remains, meaning that the anesthetist still needs to re-adjust the target effect concentration every time the observed drug effect in the patient does not match the clinically desired one. Following this trend several other strategies were recently proposed. For example, in [14] an adaptive approach is proposed to improve TCI based strategies. The method combines a optimal variance constrained drug dose design with a hybrid identification of the individual patient dynamics. The model on that study was based on the one described in Section II-B. Despite constituting a real improvement regarding the commonly used TCI strategies, the results from the tests of the algorithm on the NMB control present some inaccuracies regarding reference tracking. It is actually the patient intra and intervariabilities that plays the major role and indicates a need for new models and identification algorithms.

B. State of the art models

The model used in the previous studies to describe the PK and PD of the drug effect, in the special case of the non-depolarizing muscle relaxant *atracurium*, is presented in this subsection. This will not be the model adopted for the development of this paper, but it motivates and supports the build up of the new proposed model and identification algorithms. To meet the parsimony principle, the main design goal is then to perform the modeling with a minimal number of parameters.

Recalling the compartmental type models [15], the NMB model can be described as a Wiener model as proposed in [16]. The PK is described by the linear dynamic block 1 in Fig. 1. The

physiological basis of this part consists of assuming two plasma compartments (central and peripheric) both communicating with each other. The PD incorporates a linear dynamic part (blocks 2 and 3 in Fig. 1) and a nonlinear static block (block 4 in Fig. 1). The relation between the plasma concentration $c_p(t)$ and the effect concentration $c_e(t)$ was first described without block 3 in Fig. 1 [17] but, as shown in [18], the inclusion of this equation allows a better fit to the observed experimental responses. Block 4 in Fig. 1 represents the PD static nonlinearity and relates the effect concentration to the effect of the drug as quantified by the measured signal $r(t)$. This model depends on eigth parameters that need to be estimated from clinical data.

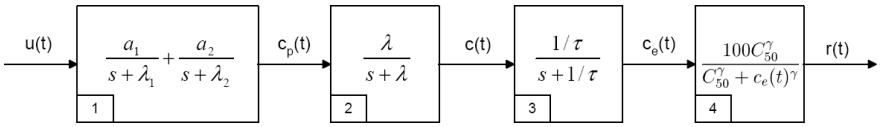

Fig. 1. Block diagram for the PK/PD of the muscle relaxant *atracurium*.

A state space description of the model of Fig. 1 is given by:

$$\begin{pmatrix} \dot{x}_1(t) \\ \dot{x}_2(t) \\ \dot{c}(t) \\ \dot{c}_e(t) \end{pmatrix} = \tag{1}$$

$$\begin{pmatrix} -\lambda_1 & 0 & 0 & 0 \\ 0 & -\lambda_2 & 0 & 0 \\ \lambda & \lambda & -\lambda & 0 \\ 0 & 0 & 1/\tau & -1/\tau \end{pmatrix} \begin{pmatrix} x_1(t) \\ x_2(t) \\ c(t) \\ c_e(t) \end{pmatrix} + \begin{pmatrix} a_1 \\ a_2 \\ 0 \\ 0 \end{pmatrix} u(t),$$

where $\{a_i\,[kg\,ml^{-1}],\ \lambda_i\,[min^{-1}]\}_{i=1,2}$, $\lambda\,[min^{-1}]$, $\tau\,[min]$ are patient-dependent parameters. In turn, $c_e(t)$ is related with the expected NMB level $r(t)\,(\%)$ by means of a nonlinear static Hill equation [17],

$$r(t) = \frac{100\, C_{50}^{\gamma}}{C_{50}^{\gamma} + c_e^{\gamma}(t)}\,, \tag{2}$$

where $C_{50}\,[\mu g\, ml^{-1}]$ and γ (dimensionless) are also patient-dependent parameters. Note that in practice the intermediate signal $c_e(t)$ is not accessible for measurement. The variable $r(t)$, normalized between 0 and 100, measures the NMB level, 0 corresponding to full paralysis and 100 to full muscular activity.

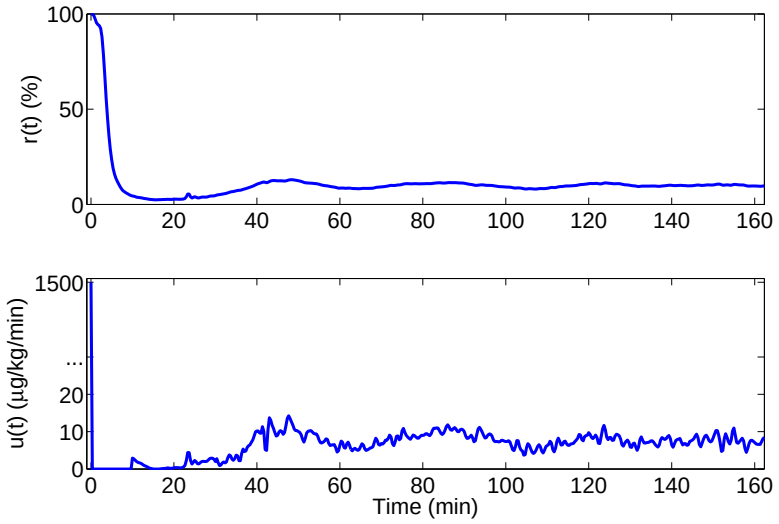

Fig. 2. NMB response (upper plot) and input drug dose (lower plot) from a real case collected in closed-loop control for the muscle relaxant *atracurium*. Note that the scale in the *y*-axis of the lower plot has been split.

Fig. 2 represents the typical response of a closed-loop controlled real case for the administration of *atracurium* in the surgery room. The output signal $r(t)$ is represented in the upper plot whereas the input drug dose $u(t)$ is shown in the lower plot. As can be seen in the lower plot, at the beginning of the surgery, in the induction phase, a *bolus* of *atracurium*, typically $u_\delta = 500\,\delta(t)\,\mu g\, kg^{-1}$ (in discrete time corresponding to $u(0) = u_\delta\,\Delta t$ with $\Delta t = 1/3 min^{-1}$) is administered to the patient to enable a rapid drop of NMB level. For control purposes, during the period where the *bolus* is acting, the value of the reference is fixed at a low level, being gradually raised to the set-point of 10% [16]. The output signal $r(t)$ represented in the upper plot of Fig. 2 was then maintained around the reference profile by the administration of the input

drug dose $u(t)$, calculated by a closed-loop control strategy [19].

As it is clear from Fig. 2 the input signal is not rich enough to make the identification of the eight parameters of the model (1), (2) possible. The poor input excitation as well as the limited experimental dataset hence motivate the present study.

III. New model: minimal number of parameters

A new SISO Wiener model describing *atracurium* PK/PD is presented in this section. Algorithms for simultaneous identification of the linear dynamics and the static non linearity are then derived. Models are first constructed using a continuous time Wiener model. This model is then sampled with a zero-order hold strategy [20]. This enables the derivation of algorithms that estimate the underlying continuous time parameters, thereby exploiting the fact that the continous time parameters are of minimal number.

A. Linear block

For simulation purposes, and in order to cover a wide range of behaviours, a bank of realistic nonlinear dynamic models for *atracurium* PK/PD have been generated using the probabilistic distribution discussed in [18]. It then constitutes a simulated database where the exact parameterization of model (1) is known for each simulated patient. Fig. 3 shows the effect concentration (output from the linear part) response from the model number 25 in the simulated bank after administration of the drug dose profile represented in Fig. 2. Despite some differences on the local behaviour of different patients' effect concentration, the global trend of the represented plot can be considered typical. A rapid raise is present at the beginning of the surgery due to the *bolus* administration, being then followed by a slower decrease to a certain level around the value corresponding to the steady-state.

By inspection of the output from the linear part in simulation, a model with an *n*th-order multiple pole located in $-1/\tau$ with unitary static gain was first proposed (3) to account for the dynamics in (1). Model order is denoted by the superscript $^{(n)}$ in the paper. For the sake of simplicity $\alpha = 1/\tau$ is defined. This gives

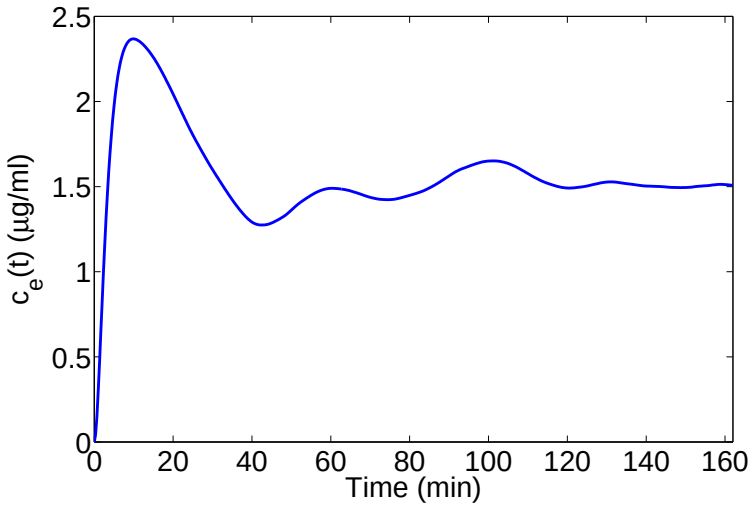

Fig. 3. Effect concentration for model number 25 in the simulated database after administration of the drug dose profile represented in Fig. 2.

$$\hat{C}_e^{(n)}(s,\alpha) = \frac{\alpha^n}{(s+\alpha)^n}\, U(s)\,, \{n = 2,3,4\}, \tag{3}$$

where $\hat{C}_e^{(n)}(s,\alpha)$ is the Laplace transform of the output from the model linear dynamic part $\hat{c}_e^{(n)}(t,\alpha)$ and $U(s)$ is the Laplace transform of the input signal $u(t)$.

However, it was hypothesized that, by placing the model poles in different locations, better accuracy could be achieved. According to [21], it is possible to describe the model dynamics using the limiting Laguerre approximations. It is this idea that is the basis for the next refinement.

Instead of having a pole with multiplicity n located in $-1/\tau$, several combinations of multiples of $-1/\tau$ are introduced for the pole locations. Hence, instead of using the linear model (3), the following **is** proposed:

$$\hat{C}_e^{(n)}(s,\alpha) = \frac{k_1 \,\ldots\, k_n\, \alpha^n}{(s+k_1\,\alpha)\ldots(s+k_n\,\alpha)}\, U(s),\ \{n = 2,3,4\}, \tag{4}$$

Aiming for the best modeling, the parameters $k_i, \{i = 2,3,4\}$ must be chosen, noting that $k_1 = 1$ needs to hold. A brute force search on the available real collected cases database was

then performed. A detailed description and some results on this are present in Section VI.

B. Nonlinear block

The output from the non-linear block was modeled with the Hill equation:

$$\hat{y}(t,\theta) = \frac{100\, C_{50}^{\gamma}}{C_{50}^{\gamma} + \hat{c}_e^{\gamma}(t,\alpha)}, \tag{5}$$

where $\theta = (\theta_1 \;\; \theta_2)^T = (\alpha \;\; \gamma)^T$.

Noting that the linear part contributes with a unit gain for the whole system, the differential static gain must be estimated by the parameter to be adapted in the non-linear part [8]. According to [10], in simulation studies on the previouly mentioned simulated database, the variability on C_{50} does not stongly affect the identification results. Hence C_{50} was kept constant during this study. γ adapts the shape or static differential gain of (5).

C. Sampling

In order to implement the proposed model structure in the identification algorithm, the continuous-time representation (3) has to be sampled. For that purpose, the system (3) was represented in a state-space form as shown in (6).

$$\begin{cases} \dot{\hat{x}}(t) &= A(\alpha)\,\hat{x}(t) + B(\alpha)\,u(t) \\ \hat{z}(t) &= C(\alpha)\,\hat{x}(t) \end{cases}, \tag{6}$$

where $u(t) \in \mathbb{R}$ is the input (piecewise constant drug dose infusion), $\hat{x}(t) \in \mathbb{R}^{n\times 1}$ the continuous model state-vector, $\hat{z}(t) \in \mathbb{R}$ is the output (effect concentration of the drug), $C(\alpha) \in \mathbb{R}^{1\times n}$, $A(\alpha) \in \mathbb{R}^{n\times n}$ and $B(\alpha) \in \mathbb{R}^{n\times 1}$, being the system matrices. Note that $k_i's$ are not shown explicitely in (6) since they are determined in a single optimization step with respect to the available data. After that, only α affects the dynamics of the different patients.

The zero-order hold method [20] was applied using the sampling instant $t_k = kh$. Normally, h is equal to 20 seconds. This choice is due to the fact that, in the surgery environment, data from NMB is acquired with a frequency of $1/20s^{-1}$. The discrete time model than becomes

$$\begin{cases} \hat{x}(kh+h) &= \Phi(\alpha)\,\hat{x}(kh) + \Gamma(\alpha)\,u(kh) \\ \hat{z}(kh) &= C(\alpha)\,\hat{x}(kh) \end{cases}, \tag{7}$$

where

$$\begin{aligned} \Phi(\alpha) &= e^{A(\alpha)h} \\ \Gamma(\alpha) &= \int_0^h e^{A(\alpha)s}\,ds\,B(\alpha) \end{aligned} \tag{8}$$

Here, $u(kh) \in \mathbb{R}$ is the input (piecewise constant drug dose infusion), $\hat{x}(kh) \in \mathbb{R}^{n\times 1}$ the discrete model state-vector, $\hat{z}(kh) \in \mathbb{R}$ is the output (effect concentration of the drug), $\Gamma(\alpha) \in \mathbb{R}^{n\times n}$ and $B(\alpha) \in \mathbb{R}^{n\times 1}$, being the sampled system matrices.

For the purpose of implementing the prediction error method, the polynomial counterpart to (7) is more suitable to use. According to [20], the pulse transfer operator corresponding to (7) is given by

$$H(q^{-1},\alpha) = C(\alpha)(qI - \Phi(\alpha))^{-1}\Gamma(\alpha) = \frac{B(q^{-1},\alpha)}{A(q^{-1}\alpha)}\,. \tag{9}$$

where q is the shift operator ($qu(kh) = u(kh+h)$).

The model output from the linear part can then be represented as

$$\hat{c}_e^{(n)}(t,\alpha) = \frac{B(q^{-1},\alpha)}{A(q^{-1},\alpha)}\,u(t)\,. \tag{10}$$

The sampling does not affect the nonlinear block, hence (5) can be used as it is.

IV. Batch identification algorithm: Prediction Error Method

The linear dynamics and static nonlinearity will be jointly identified. Let

$$\theta = (\theta_1 \quad \theta_2)^T = (\alpha \quad \gamma)^T \tag{11}$$

denote the parameter vector to be identified, where α is the parameter of the linear block and γ the parameter of the nonlinearity.

The prediction error method determines θ so that the prediction error

$$\varepsilon(t,\theta) = y(t) - \hat{y}(t,\theta). \tag{12}$$

becomes as small as possible. Note that $y(t)$ is the measured output value and $\hat{y}(t,\theta)$ is the predicted output, based on parameter vector θ.

A. Gradient

The gradient of the prediction error (12) is of central importance to the prediction error identification method. It is given by:

$$\begin{aligned}
\psi(t,\theta) &= -\left(\frac{\partial\varepsilon(t,\theta)}{\partial\theta}\right)^T \\
&= \left(\frac{\partial\hat{y}(t,\theta)}{\partial\theta}\right)^T \\
&= \left(\frac{\partial\hat{y}(t,\theta)}{\partial\alpha} \qquad \frac{\partial\hat{y}(t,\theta)}{\partial\gamma}\right)^T \\
&= \left(\frac{\partial\hat{y}(t,\theta)}{\partial\hat{c}_e(t,\alpha)}\frac{\partial\hat{c}_e(t,\alpha)}{\partial\alpha} \qquad \frac{\partial\hat{y}(t,\theta)}{\partial\gamma}\right)^T.
\end{aligned} \tag{13}$$

B. Criterion and search direction

In order to derive the prediction error method, the following criterion is introduced [12]:

$$V(\theta) = \frac{1}{N}\sum_{t=1}^{N}\varepsilon^2(t,\theta), \tag{14}$$

where N is the total number of data points and $\varepsilon(t,\theta)$ is the prediction error.

The minimization of (14) is then performed using the numerical *Gauss-Newton* method [12]:

$$\hat{\theta}^{(k+1)} = \hat{\theta}^{(k)} - \beta_k[V''(\hat{\theta}^{(k)})]^{-1}\,V'(\hat{\theta}^{(k)})^T, \tag{15}$$

where $\hat{\theta}^{(k)}$ denotes the kth iteration in the search. The sequence of scalars β_k is used to control the step lenght. The derivatives of $V(\theta)$ can be found as:

$$V'(\theta) = -\frac{2}{N}\sum_{t=1}^{N} \varepsilon^T(t,\theta)\,\psi^T(t,\theta)\,, \tag{16}$$

$$\begin{aligned} V''(\theta) &= \frac{2}{N}\sum_{t=1}^{N} \psi(t,\theta)\ \psi^T(t,\theta) \\ &\quad + \frac{2}{N}\sum_{t=1}^{N} \varepsilon(t,\theta)\ \frac{\partial}{\partial\theta}\psi^T(t,\theta) \\ &\approx \frac{2}{N}\sum_{t=1}^{N} \psi(t,\theta)\ \psi^T(t,\theta) \end{aligned} \tag{17}$$

The approximation in (17) is justified in [12] and is supported by the fact that, at the global minimum point $\varepsilon(t,\theta)$ becomes assymptotically white noise which is independent of $\psi(t,\theta)$. As a consequence, the *Gauss-Newton* method has a linear convergence instead of quadratic, which would be the case if the approximation had not been performed (*i.e.* using the *Newton-Raphson* method).

C. Projection algorithm

Regarding the linear block of the Wiener model in study, the application of a projection algorithm is needed to keep the model assymptotically stable. For that purpose, the poles of the transfer function (10) are monitored by the use of the following projection algorithm for the parameter α:

$$\alpha^{(k+1)} = \theta_1^{(k+1)} = \begin{cases} \alpha^{(k+1)} & \text{if} \quad \alpha^{(k+1)} > \delta > 0 \\ \alpha^{(k)} & \text{if} \quad \alpha^{(k+1)} \leq \delta \end{cases} \tag{18}$$

For the nonlinear block (5), it is necessary to assure that γ does not reach negative values. The following projection algorithm was used for the parameter γ:

$$\gamma^{(k+1)} = \theta_2^{(k+1)} = \begin{cases} \gamma^{(k+1)} & \text{if} \quad \gamma^{(k+1)} > \delta > 0 \\ \gamma^{(k)} & \text{if} \quad \gamma^{(k+1)} \leq \delta \end{cases} \tag{19}$$

Both updatings are hence stopped if the new parameter updates are outside the allowable range.

D. Prediction error algorithm

The Prediction error algorithm can now be summarized using the formulas defined above. Note that a numerical differentiation is used. The reason is that the mathematical expressions for the derivatives of (10) with respect to α become very complicated.

$for\ k = 0\ to\ K$

$$\hat{\theta} = \hat{\theta}^{(k)}$$

$$\hat{c}_e(t, \hat{\alpha}) = \frac{B(q^{-1}, \hat{\alpha})}{A(q^{-1}, \hat{\alpha})}\, u(t)$$

$$\hat{y}(t, \hat{\theta}) = \frac{100 C_{50}^{\hat{\gamma}}}{C_{50}^{\hat{\gamma}} + \hat{c}_e^{\hat{\gamma}}(t, \hat{\alpha})}$$

$$\varepsilon(t, \hat{\theta}) = y(t) - \hat{y}(t, \hat{\theta})$$

$$\frac{\partial \hat{y}(t, \hat{\theta})}{\partial \hat{c}_e(t, \hat{\alpha})} = -\frac{100\, C_{50}^{\hat{\gamma}}\, \hat{\gamma}\, \hat{c}_e(t, \hat{\alpha})^{\hat{\gamma}-1}}{\left(C_{50}^{\hat{\gamma}} + \hat{c}_e(t, \hat{\alpha})^{\hat{\gamma}}\right)^2}$$

$$\frac{\partial \hat{c}_e(t, \hat{\alpha})}{\partial \hat{\alpha}} = \frac{\hat{c}_e(t, \hat{\alpha} + \Delta\hat{\alpha}) - \hat{c}_e(t, \hat{\alpha})}{\Delta\hat{\alpha}}$$

$$\frac{\partial \hat{y}(t,\hat{\theta})}{\partial \hat{\gamma}} = \frac{100\, C_{50}^{\hat{\gamma}}\, ln(C_{50})}{C_{50}^{\hat{\gamma}} + \hat{c}_e(t,\hat{\alpha})^{\hat{\gamma}}} - \frac{100\, C_{50}^{\hat{\gamma}}}{\left(C_{50}^{\hat{\gamma}} + \hat{c}_e(t,\hat{\alpha})^{\hat{\gamma}}\right)^2}$$

$$\times [ln(C_{50})\, C_{50}^{\hat{\gamma}} + ln(\hat{c}_e(t,\hat{\alpha}))\, \hat{c}_e(t,\hat{\alpha})^{\hat{\gamma}}]$$

$$\psi(t,\hat{\theta}) = \left(\frac{\partial \hat{y}(t,\hat{\theta})}{\partial \hat{c}_e(t,\hat{\alpha})} \frac{\partial \hat{c}_e(t,\hat{\alpha})}{\partial \hat{\alpha}} \qquad \frac{\partial \hat{y}(t,\hat{\theta})}{\partial \hat{\gamma}} \right)^T$$

$$V'(\hat{\theta}) = -\frac{2}{N} \sum_{t=1}^{N} \varepsilon^T(t,\hat{\theta})\, \psi^T(t,\hat{\theta})$$

$$V''(\hat{\theta}) \approx \frac{2}{N} \sum_{t=1}^{N} \psi(t,\hat{\theta})\, \psi^T(t,\hat{\theta})$$

$$\hat{\theta}^{(k+1)} = \hat{\theta}^{(k)} - \beta_k [V''(\hat{\theta}^{(k)})]^{-1}\, V'(\hat{\theta}^{(k)})^T. \tag{20}$$

end

The step $\Delta\hat{\alpha}$ used for the differentiation is selected to be small.

V. Recursive identification algorithm: Extended Kalman Filter

In order to enable the incorporation of a nonlinear identification algorithm in an online platform for control of NMB, recursive identification methodologies need to be developed. This is e.g. a prerequisite when adaptive control is introduced [22]. The Extended Kalman Filter (EKF) is then a natural choice since it is well suited for adaptive control structures like Model Predictive Control (MPC). Moreover, depending on its formulation, it also provides values for the state estimates in every iteration step, these being needed for MPC control. The idea of the EKF is to

use the Kalman filter [23] for a nonlinear problem. The EKF, in contrast to the Kalman filter for linear systems, is not an optimal filter. Neverthless, it constitutes a powerful tool for recursively identifying the model parameters. In contrast to other recursive identification techniques, it also has the advantage of independent tuning using the covariance matrix of both the process and measurement noise, thereby enabling a tuning of the speed of convergence for each parameter separately. For EKF purposes, the general discrete non linear model is

$$\begin{aligned} \hat{x}(t+1) &= f(t,\hat{x}(t),u(t)) + g(t,\hat{x}(t))\,v(t) \\ \hat{y}(t) &= h(t,\hat{x}(t)) + e(t)\,, \end{aligned} \tag{21}$$

where $v(t)$ and $e(t)$ are mutually independent Gaussian white noise sequences with zero means and covariances $R_1(t)$ and $R_2(t)$, respectively. The EKF algorithm can then be summarized as follows [23]:

$$\begin{aligned} H(t) &= \left.\frac{\partial h(t,x)}{\partial x}\right|_{x=\hat{x}(t|t-1)} \\ K(t) &= P(t|t-1)H^T(t) \\ &\quad \times[H(t)P(t|t-1)H^T(t) + R_2(t)]^{-1} \\ \hat{x}(t|t) &= \hat{x}(t|t-1) + K(t)[y(t) - h(t,\hat{x}(t|t-1))] \\ P(t|t) &= P(t|t-1) - K(t)H(t)P(t|t-1) \\ \hat{x}(t+1|t) &= f(t,\hat{x}(t|t),u(t)) \\ F(t) &= \left.\frac{\partial f(t,x)}{\partial x}\right|_{x=\hat{x}(t|t)} \\ G(t) &= g(t,x)\big|_{x=\hat{x}(t|t)} \\ P(t+1|t) &= F(t)P(t|t)F^T(t) + G(t)R_1(t)G^T(t) \end{aligned} \tag{22}$$

In the next subsection, the recursive identification setting of the EKF is derived.

A. Model structural aspects

To enable the estimation of the model parameters with the EKF, a coupled identification model must be defined. The model merges the sampled model (7) and a random walk model for the parameter estimate [12]:

$$\hat{\overline{x}}(kh+h) \;=\; \begin{pmatrix} \overline{x}_1(kh+h) \\ \vdots \\ \hat{\overline{x}}_n(kh+h) \\ \hat{\overline{x}}_{n+1}(kh+h) \\ \hat{\overline{x}}_{n+2}(kh+h) \end{pmatrix} = \begin{pmatrix} x_1(kh+h) \\ \vdots \\ \hat{x}_n(kh+h) \\ \hat{\theta}_1(kh+h) \\ \hat{\theta}_2(kh+h) \end{pmatrix}. \tag{23}$$

Hence, the extended state-space model is the following:

$$
\begin{aligned}
\hat{\overline{x}}(kh+h) &= \begin{pmatrix} \Phi(\alpha) & \begin{matrix} 0 & 0 \\ 0 & 0 \end{matrix} \\ \begin{matrix} 0 & 0 \\ 0 & 0 \end{matrix} & I \end{pmatrix} \begin{pmatrix} \hat{x}(kh) \\ \hat{\theta}(kh) \end{pmatrix} + \\
&\quad + \begin{pmatrix} \Gamma(\alpha) \\ 0 \\ 0 \end{pmatrix} u(kh) + \begin{pmatrix} I & \begin{matrix} 0 & 0 \\ 0 & 0 \end{matrix} \\ \begin{matrix} 0 & 0 \\ 0 & 0 \end{matrix} & I \end{pmatrix} w(kh) \\
&\equiv \begin{pmatrix} f_1(kh, \hat{\overline{x}}(kh), u(kh)) \\ f_2(kh, \hat{\overline{x}}(kh), u(kh)) \\ \vdots \\ f_{n+2}(kh, \hat{\overline{x}}(kh), u(kh)) \end{pmatrix} + g\, w(kh) \\
&\equiv f(kh, \hat{\overline{x}}(kh), u(kh)) + g\, w(kh) \qquad (24)
\end{aligned}
$$

$$
\begin{aligned}
\hat{y}(kh) &= \frac{100\ C_{50}^{\hat{\overline{x}}_{n+2}(kh)}}{C_{50}^{\hat{\overline{x}}_{n+2}(kh)} + (\overline{C}(\alpha)\hat{\overline{x}}(kh))^{\hat{\overline{x}}_{n+2}(kh)}} \\
&\equiv h(kh, \hat{\overline{x}}(kh)) + e(kh)\,. \qquad (25)
\end{aligned}
$$

$$
\overline{C}(\alpha) = \begin{pmatrix} C(\alpha) & 0 & 0 \end{pmatrix} \qquad (26)
$$

B. Linearization

In the EKF algorithm structure (22), it is necessary to linearize both $f(t,x)$ and $h(t,x)$.

The linearization of $f(kh, \hat{\overline{x}}(kh), u(kh))$ was performed analytically. The formula for $F(kh)$ is not shown here due to its complexity.

The linearization of $h(kh, \hat{\overline{x}}(kh))$ (24) was performed numerically:

$$\begin{aligned} H(kh) &= \frac{\partial h(kh, \hat{\overline{x}}(kh))}{\partial \hat{\overline{x}}(kh)} \\ &= \frac{h(kh, \hat{\overline{x}}(kh) + \Delta\hat{\overline{x}}(kh)) - h(kh, \hat{\overline{x}}(kh))}{\Delta\hat{\overline{x}}(kh)}, \end{aligned} \tag{27}$$

where $\Delta\hat{\overline{x}}(kh)$ is the step for the differentation and chosen to be small.

C. Algorithm and Initialization

After having formulated all the quantities needed to set up the EKF, the initial values for the variables must be specified. For the third order model, the initial values for the states were

$$\hat{\overline{x}}(0|-1) = (0.000 \quad 0.000 \quad 0.000 \quad 0.030 \quad 1.000)^T \tag{28}$$

Using simulations performed on the available database, it was found that, the matrix $P(t|t-1)$ could be initialized as:

$$P(0|-1) = \begin{pmatrix} 1 & 0 & 0 & 0 & 0 \\ 0 & 0.01 & 0 & 0 & 0 \\ 0 & 0 & 0.0001 & 0 & 0 \\ 0 & 0 & 0 & 0.1 & 0 \\ 0 & 0 & 0 & 0 & 1 \end{pmatrix} \tag{29}$$

Performing a similar empirical analysis on the simulated signals, the values for the covariance matrices R_1 and R_2 were set to:

$$R_1 = \begin{pmatrix} 10^2 & 0 & 0 & 0 & 0 \\ 0 & 1^2 & 0 & 0 & 0 \\ 0 & 0 & 0.1^2 & 0 & 0 \\ 0 & 0 & 0 & 1^2 & 0 \\ 0 & 0 & 0 & 0 & 100^2 \end{pmatrix} \quad (30)$$

$$R_2 = 10^8 \quad (31)$$

VI. Optimization of the pole location for the new model

For the remaining parts of this paper, model order $n = 3$ in (4) and (23) was chosen. Tests for $n = 2, 3, 4$ were performed (results not shown) and $n = 3$ proved to give better results concerning the fitting of the system output signal.

In order to choose a combination of $k_i's$ (Section III-A) that leads to the best identification results, the PEM described in Section IV-D was applied to the signals from the sixty real collected cases present in the available database. The signal time window for evaluation (of lenght M) started on minute 30 (after the transient phase where the *bolus* is acting) and stopped at the end of the infusion ($t = t^*$). For the same patient, a combination of (k_2, k_3) ranging from $k_i = 1$ to $k_i = 10, \{i = 2, 3\}$ was tested. The same procedure was applied to every patient. The number of total algorithm iterations in each trial was 1000, to ensure convergence of the identified parameters. The normalized sum of the squared prediction error $\varepsilon(t, \hat{\theta})$ for each combination (k_2, k_3) and for each identified patient j was calculated:

$$\varepsilon_j(k_2, k_3) = \frac{1}{M} \sum_{t=31min}^{t^*} \left(\varepsilon(t, \hat{\theta})\right)^2 . \quad (32)$$

To perform a statistical analysis of the results coming from simulations with different (k_2, k_3) combinations, a normalized sum among the total number of patients was calculated to obtain a single performance error value $\Psi(k_2, k_3)$ for each (k_2, k_3) combination:

$$\Psi(k_2, k_3) = \frac{1}{60} \sum_{j=1}^{60} \varepsilon_j(k_2, k_3) \tag{33}$$

A graphical representation of the $\Psi(k_2, k_3)$ behaviour in three-dimensional space is shown in Fig. 4.

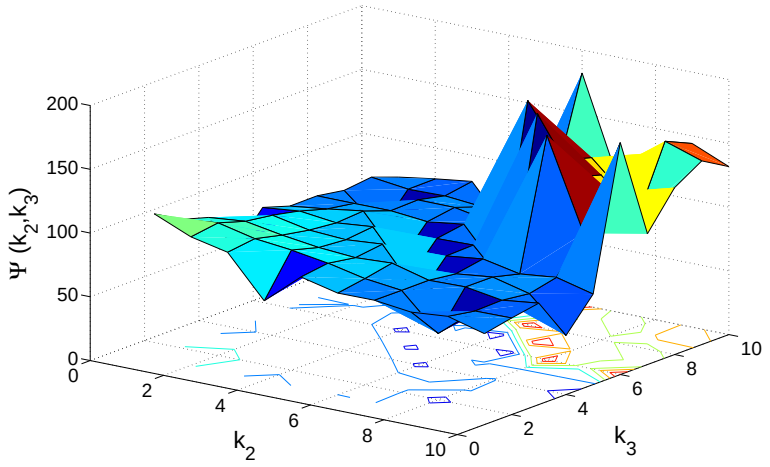

Fig. 4. Normalized performance error values for all combinations of (k_2, k_3) from 1 to 10. The values come from simulations with a third-order model (4) in the database of sixty real patients with the PEM described in Section IV.

By analyzing the surface in Fig. 4 it was found that the minimum normalized error for each (k_2, k_3) combination in the patient database appeared for $k_2 = 4$ and $k_3 = 10$ or vice-versa. From here on, all the tests performed on the database will use these values for k_2 and k_3.

The real case presented in Fig. 2 was used to exemplify the performance of the PEM for a minimally parameterized model. A third order model was used to describe the linear part (4). The results of the simulated output signal together with the real measured signal are presented in Fig. 5. The simulated effect concentration $\hat{c}_e(t, \hat{\theta})$, *i.e.* the output from the linear block, is represented in Fig. 6. Note that, as mentioned before, this effect concentration is scaled when compared with the one in Fig. 3 due to the fact that the system total gain is only adjusted by the parameter from the nonlinear block. However, the signal behaviour in Fig. 6 follows the same pattern as the one in Fig. 3, showing that the strategy of representing the system by a minimally

parameterized model was successful. The algorithm was initialized with

$$\hat{\theta}^{(0)} = (0.500 \quad 2.000)^T. \tag{34}$$

The chosen value for β_k in (15) was:

$$\beta_k = \begin{pmatrix} 0.1 & 0 \\ 0 & 1 \end{pmatrix} \tag{35}$$

After 1000 samples, the following estimates were obtained:

$$\hat{\theta}^{(1000)} = (0.036 \quad 2.688)^T. \tag{36}$$

The result is illustrated in Fig. 7. These figures show that the algorithm manages to produce parameter estimates such that the simulated signal $\hat{y}(t, \hat{\theta}_{1000})$ calculated with the parameter estimates obtained at the end of the run and the real output signal $y(t)$ almost coincide. The initial drop in $y(t)$ was modeled by the simulated signal and the recovery of the simulated signal coincides with the recovery of the real signal. Most importantly, it should be stressed that the simulated output captured the oscillations that are present in the real signal $y(t)$.

VII. EKF Performance Evaluation

The purpose of the following section is to illustrate the practical performance of the EKF algorithm for the model in (24) that describes the effect of the neuromuscular relaxant *atracurium*. Simulations were performed using the real collected NMB cases in the database.

The EKF simulated output signal $\hat{y}(t, \hat{\theta})$ and the real measured NMB output signal $y(t)$ are illustrated in Fig. 8. The results show that the simulated signal follows the real output throughout time, catching the behaviour of the measured signal in both the initial *bolus* response, and the recovery, transient and steady-state phases. The algorithm was able to discard the noise effects

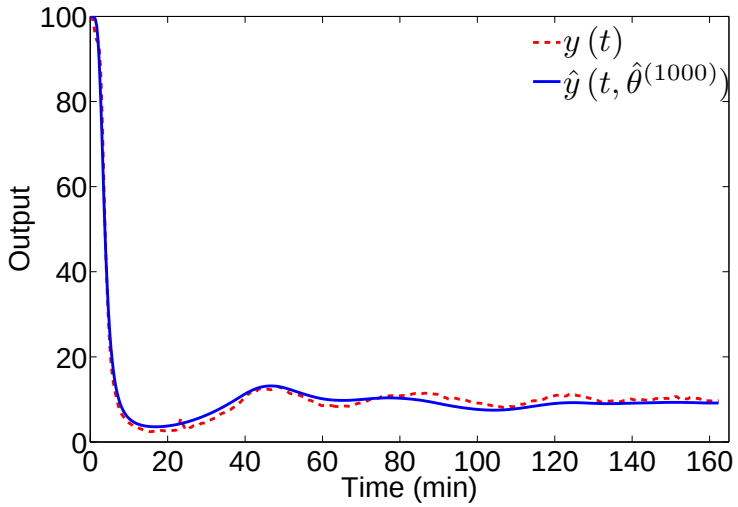

Fig. 5. The real measured NMB data (in dashed line) plotted together with the simulated output model response (in solid line), using the parameter estimates obtained at the end of the PEM run.

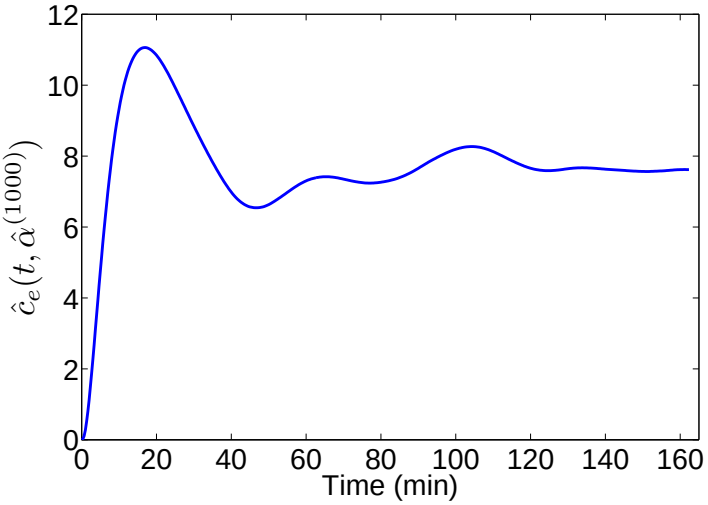

Fig. 6. The simulated (scaled) effect concentration $\hat{c}_e(t,\hat{\alpha}^{(1000)})$, using the parameter estimates obtained at the end of the PEM run.

present in the measured NMB signal, giving raise to a filtered signal able to follow the real signal time evolution. This behaviour is due to the parameter estimates update provided by the EKF algorithm. The evolution in time of the updated parameters $\hat{\alpha}$ and $\hat{\gamma}$ are illustrated in Fig. 9 and 10, respectively. At the beginning of the simulation there is a significant change in the updates in every iteration. However, afterwards the estimates stabilize. Despite the initial estimates for

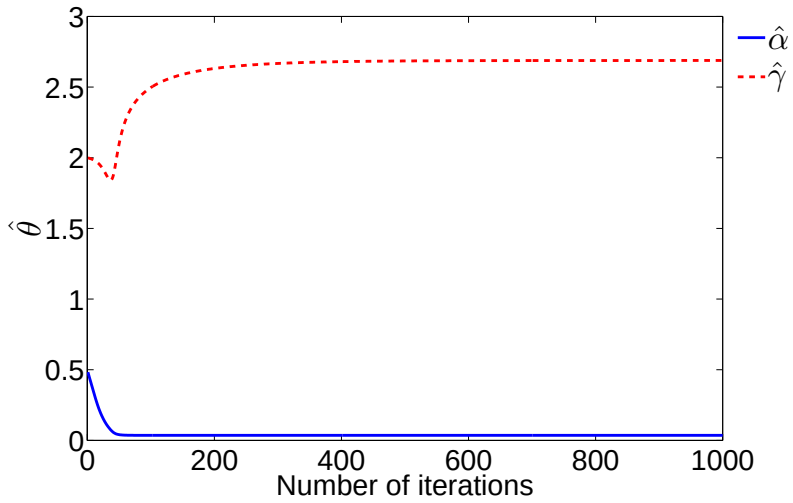

Fig. 7. The parameter estimates generated by the PEM.

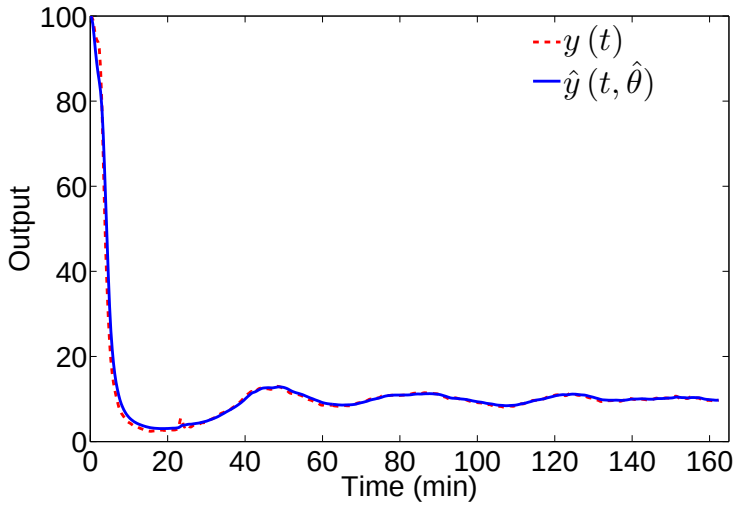

Fig. 8. The real measured NMB data (in dashed line) plotted together with the simulated output model response (in solid line), using the parameter estimates updated by the EKF algorithm.

both parameters are far from the final ones, the algorithm proved to be able to adapt both $\hat{\alpha}$ and $\hat{\gamma}$. (Interestingly, the median values of both parameter estimates calculated with the EKF approach are near the final estimates in the PEM run (36).)

It can be concluded from the plots that the proposed EKF algorithm is capable of accurately identifying the newly proposed Wiener model structure, minimally parameterized, for the drug

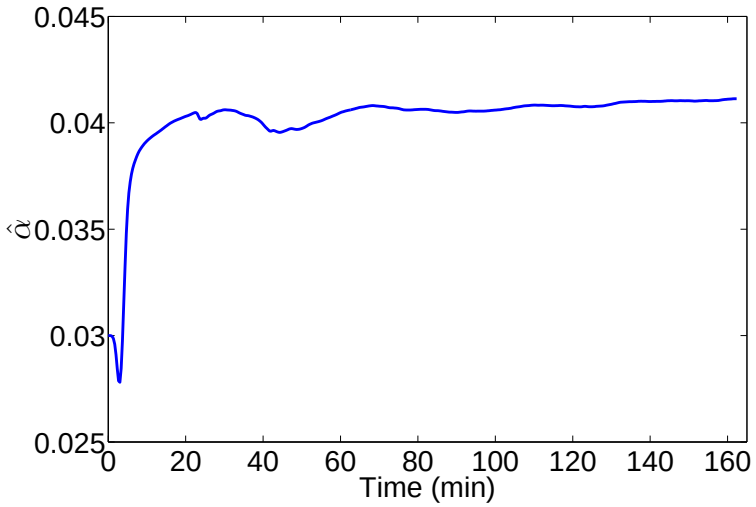

Fig. 9. The estimates of parameter α updated by the EKF algorithm.

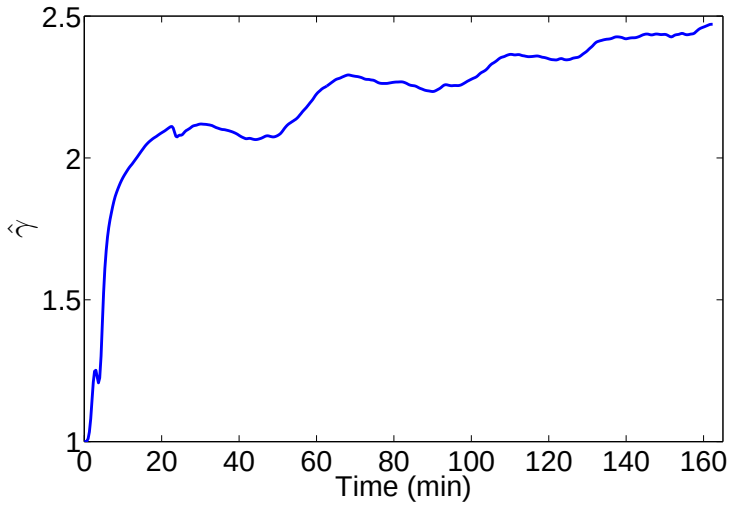

Fig. 10. The estimates of parameter γ updated by the EKF algorithm.

effect in the NMB case study.

VIII. Conclusion

The paper has presented a new strategy of modeling and identifying overparameterized physiological models. The example of NeuroMuscular Blockade level was used. The newly developed minimally parameterized Wiener model for the effect of the muscle relaxant *atracurium* proved

to satisfactory describe the output signal behaviour of the system. System identification strategies were also developed for the new proposed model.

The most commonly used SISO model describing the effect of the muscle relaxant *atracurium* relies on eight parameters to be identified. The major drawback for the application of system identification techniques for the identification of such a number of parameters is due to the presence of poor input excitation and lack of enough available output data. To overcome these two issues, a new third-order model was proposed with only two parameters to be identified. A batch Prediction Error Method was first developed to optimize the model structure. Secondly, a Extended Kalman Filter was derived, aiming for the development of online system identification routines to be implemented in control devices. Both system identification approaches showed good results regarding parameter adaptation and measured signal tracking. Thus, the newly proposed method proved to be adequate for the description of the system, even for the input signal present in this case study.

These results point to the possiblility of further work on system identification techniques for minimally parameterized models in anaesthesia, namely the adaptation of these algorithms to the DoA case, using the BIS signal. Further studies on initialization algorithms as well as on the convergence properties of the developed methods are also recommended to ensure a safe incorporation of such system identification strategies in anaesthesia integrated control platforms.

ACKNOWLEDGMENT

The authors would like to thank Fundação para a Ciência e Tecnologia who partially funded the research present on this paper through the project IDeA - Integrated Design for Automation in Anaesthesia (reference PTDC/EEA- ACR/69288/2006). The stipend given by the Bernt Järmarks foundation for scientific research is also gratefully acknowledged.

REFERENCES

[1] G. Widman, T. Schreiber, B. Redhberg, A. Hoeft, and C. E. Elger, “Quantification of depth of anesthesia by nonlinear time series analysis of brain electrical activity,” *Physical Review*, vol. 62, no. 4, pp. 4898–4903, 2000.

[2] M. M. R. F. Struys, E. W. Jensen, W. Smith, N. T. Smith, I. Rampil, F. J. E. Dumortier, C. Mestach, and E. P. Mortier, "Performance of the arx-derived auditory evoked potential index as an indicator of anesthetic depth: A comparison with bispectral index and hemodynamic measures during propofol administration," *Anesthesiology*, vol. 96, pp. 803–816, 2002.

[3] J. Bruhn, H. Röpcke, and A. Hoeft, "Approximate entropy as an electroencephalographic measure of anesthetic drug effect during desflurane anesthesia," vol. 92, pp. 715–726, 2000.

[4] P. S. Glass, M. Bloom, L. Kearse, C. Rosow, P. Sebel, and P. Manberg, "Bispectral analysis measures sedation and memory effects of propofol, midazolam, isoflurane, and alfentanil in healthy volunteers," *Anesthesiology*, vol. 86, pp. 836–847, 1997.

[5] S. Schraag, "Theoretical basis of target controlled anaesthesia: history, concept and clinical perspectives," *Best Practice and Research Clinical Anaesthesiology*, vol. 15, no. 1, pp. 1–17, 2001.

[6] H. Alonso, T. Mendonça, J. M. Lemos, and T. Wigren, "A simple model for the identification of drug effects," in *Proc. IEEE International symposium on Intelligent Signal Processing (WISP'09)*, Budapest, Hungary, 2009, pp. 000–000.

[7] T. Wigren, "User choices and model validation in system identification using nonlinear wiener models," in *Proc. of the 13th IFAC Symposium on System Identification*, Rotterdam, the Netherlands, 2003, pp. 863–868.

[8] ——, "Recursive prediction error identification method using the nonlinear Wiener model," *Automatica*, vol. 29, no. 4, pp. 1011–1025, 1993.

[9] H.-H. Lin, C. L. Beck, and M. J. Bloom, "On the use of multivariable piecewise-linear models for predicting human response to anesthesia," *IEEE Trans. Biomed. Eng.*, pp. 1876–1887, Nov. 2004.

[10] H. Alonso, T. Mendonça, and P. Rocha, "A hybrid method for parameter estimation and its application to biomedical systems," *Computer Methods and Programs in Biomedicine*, vol. 89, pp. 112–122, 2008.

[11] T. Wigren, *MATLAB software for Recursive Identification of Wiener Systems - Revision 2*. Uppsala, Sweden: Uppsala University, 2007.

[12] T. Söderström and P. Stoica, *System Identification*. Hemel Hempstead, UK: Prentice-Hall, 1989.

[13] *Diprifusor: Target Controlled Infusion (TCI) in anaesthetic practice*, AstraZeneca, Alderley House, Alderley Park, Macclesfield, Chechire, UK, 1999.

[14] M. M. Silva, H. Alonso, J. M. Lemos, and T. Mendonça, "An adaptive approach to target controlled infusion," in *Proc. European Control Conference (ECC'09)*, Budapest, Hungary, 2009, pp. 000–000.

[15] K. Godfrey, *Compartmental models and their application*. Academic Press, 1983.

[16] T. Mendonça and P. Lago, "PID control strategies for the automatic control of neuromuscular blockade," *Control Engineering Practice*, vol. 6, no. 10, pp. 1225–1231, 1998.

[17] B. Weatherley, S. Williams, and E. Neill, "Pharmacokinetics, pharmacodynamics and dose-response relationships of atracurium administered i. v." *Br. J. Anaesth.*, vol. 55, pp. 39s–45s, 1983.

[18] P. Lago, T. Mendonça, and L. Gonçalves, "On-line autocalibration of a pid controller of neuromuscular blockade," in *Proc. of the 1998 IEEE International Conference on Control Applications*, Trieste, Italy, 1998, pp. 363–367.

[19] M. M. da Silva, T. Mendonça, and S. Esteves, "Personalized neuromuscular blockade through control: clinical and technical evaluation," in *Proc. of the 30th Anual International Conference of the IEEE Engineering in Medicine and Biology Society*, Vancouver, Canada, 2008, pp. 5826–5829.

[20] K. J. Åström and B. Wittenmark, *Computer-Controlled Systems*. Englewood Cliffs, NJ: Prentice Hall, 1984.

[21] B. Wahlberg, "System identification using laguerre models," *IEEE Trans. Autom. Control*, pp. 551–562, Jan. 1991.

[22] K. J. Åström and B. Wittenmark, *Adaptive Control*. Reading, MA: Addison-Wesley, 1989.

[23] T. Söderström, *Discrete-time Stochastic Systems*. London, UK: Springer-Verlag, 2002.

PLACE PHOTO HERE

Margarida Martins da Silva was born in Fundão, Portugal, in 1984. She received the M.Sc. degree in biomedical engineering from Instituto Superior Técnico, Universidade Técnica de Lisboa, in 2007. She is currently a research assistant at Departamento de Matemática Aplicada, Faculdade de Ciências, Universidade do Porto, Portugal. Her interests are in the area of modeling, identification and control, in particular applied to biomedical systems.

PLACE PHOTO HERE

Torbjörn Wigren (S'89-M'91-SM'98) received the M.Sc. degree (engineering physics) in 1985 and the Ph.D degree (automatic control) in 1990, both from Uppsala University, Uppsala, Sweden. Since 2000 he has held positions as adjunct professor of automatic control and adjunct professor of systems modeling, at Uppsala University. He is employed by Ericsson AB, Stockholm, Sweden, where he works with signal processing for the WCDMA uplink. In 2007, he received the Ericsson Inventor of the Year award for work on High Speed Uplink Packet Access (HSUPA) technology. He received the DARPA coin for cellular location related work in 2003. His main technical interests include radio signal processing, as well as identification, estimation and control of nonlinear systems.

PLACE PHOTO HERE

Teresa Mendonça (M'03) was born in Porto, Portugal. She received the applied mathematics degree and the Ph.D. degree in applied mathematics (systems theory and signal processing) from Faculdade de Ciências da Universidade do Porto (FCUP), Portugal, in 1993. She is currently an Auxiliar Professor in the Department of Applied Mathematics at FCUP and Researcher in the Mathematical Systems Theory Group, UI&D Matemática e Aplicações, Universidade de Aveiro, Portugal. Her research interests are in the area of control systems, in particular, applied to biomedical systems. She has been involved in projects on modeling and control of anaesthesia area.